RSC Advances

PAPER

View Article Online
View Journal | View Issue

Cite this: *RSC Adv.*, 2024, **14**, 373

Intermolecular interactions in mixed dye systems and the effects on dye wastewater treatment processes

Daniu Cai,[a] Yingwu Zhang,[a] Jianyang Li,[b] Dongliang Hu,[b] Minggong Wang,[a] Guangcai Zhang[a] and Junsheng Yuan*[a]

Dye wastewater discharge is a critical concern across textiles, paper, cosmetics, and other industries. This study explores the impact of dye–dye interactions on chemical coagulation and ultrafiltration process. Using basic and reactive dyes, representing cationic and anionic compounds, the intricate interplay between these dyes was examined through spectroscopic analysis. Remarkably, interactions between dyes of opposite charges exhibited significant effects on both techniques. Electrostatic attractions played a key role. Positive coagulant hydrolysates selectively attracted negative dyes, while negatively charged membranes effectively captured positive dyes. Combining dyes with opposite charges resulted in enhanced removal efficiency, addressing challenging dyes collectively. This discovery offers a novel approach to improving dye removal, utilizing opposite-charged dye mixtures can tackle stubborn dyes unmanageable by conventional methods.

Received 16th March 2023
Accepted 7th November 2023

DOI: 10.1039/d3ra01733h

rsc.li/rsc-advances

1. Introduction

The discharge of dye wastewater is one of the most serious environmental problems currently faced by textile manufacturing, paper, cosmetics, leather tanning, and pharmaceutical industries. About 15% of the total world dye production is lost during the dyeing process and is released into industrial liquid effluents.[1] Dye molecules are mostly aromatic compounds with complex structures that are difficult to biodegrade.[2] If dye wastewater is discharged into the water body without appropriate treatment, it can lead to serious problems such as eutrophication of water bodies, reduced photosynthesis of aquatic plants, and human chromosomal aberrations caused by the accumulation of dye molecules in the food chain.[3,4]

Several treatment techniques have been widely applied in engineering for the removal of dyes from wastewater, including chemical coagulation/flocculation, adsorption, and membrane separation. Chemical coagulation has been commonly used either as a main or pre-treatment due to its low capital cost. It involves the addition of chemicals to alter the physical state of dissolved and suspended dyes and facilitates their removal by sedimentation. Its main drawbacks are the generation of sludge and ineffective decolorization of soluble dyes.[5,6] Membrane separation, including ultrafiltration, nanofiltration, and reverse osmosis, is an advanced technology for dye wastewater treatment. In this process, dye contaminants are trapped by porous membranes, while water is allowed to pass through. Therefore, it can be used for the recovery of water resources. However, high cost and frequent membrane fouling limit its application.[2,7] The adsorption method is based on the affinity of various dyes for adsorbents. It is simple and efficient, but the regeneration of adsorbents and the eco-friendly disposal of spent adsorbents must be considered.[8,9] There are also novel technologies, such as advanced oxidation processes, bio-electrochemical degradation, and photocatalytic degradation, which have been developed and are constantly being improved.[7]

Although there have been numerous studies on dye removal from aqueous solutions, most of the dye solutions tested in these studies have a relatively simple composition. Particularly when testing emerging technologies, an aqueous solution containing only a single dye is often used for convenience. In fact, real industrial dye wastewater is complex, as it contains a mixture of multiple dyes of different classes and various chemical additives. However, the removal of dye from industrial effluents containing more than one dye has not been extensively studied.[5,10] Moreover, to the best of our knowledge, little research has focused on investigating the intermolecular interactions of different classes of dyes in industrial effluents, or the effects of these interactions on the removal of dyes by certain treatment techniques.

In this study, the intermolecular interactions between dyes with both opposite and the same charge were investigated through spectroscopic measurements. Basic dyes and reactive dyes were selected as representative water-soluble cationic and anionic dyes, respectively, which are widely applied in textile,

[a]College of Chemical Engineering and Material, Quanzhou Normal University, Quanzhou 362000, Fujian, China. E-mail: jsyuan2012@126.com
[b]Qingyuan Jingong Environmental Protection Technology Co., Ltd, Quanzhou 362200, Fujian, China

printing, paper, and other industries. Two common dye removal techniques, chemical coagulation and ultrafiltration, were used for the treatment of single- and mixed-dye systems, respectively. By comparing the removal of dyes before and after mixing, the mechanism of the effect of intermolecular interactions between dyes on the treatment process was proposed.

2. Materials and methods

2.1 Reagents

A cationic dye, basic blue 22 (BB22), and an anionic dye, reactive yellow 86 (RY86), were purchased from commercial suppliers in Shanghai, China. The structural formulas of the dyes are presented in Fig. 1. Polyaluminum chloride (PAC) was purchased as commercial grade, and magnesium chloride ($MgCl_2$) and anionic polyacrylamide (APAM) were purchased as reagent grade. Ultrafiltration membrane films made of polyethersulfone (PES) with molecular weight cutoffs (MWCOs) of 5 kDa, 10 kDa, and 30 kDa were provided by Dow/Filmtec, USA. The pH adjustment was performed using NaOH and HCl, which were of reagent grade. Deionized water was prepared using reverse osmosis and was used as solvent throughout.

2.2 UV-visible spectral measurements

The spectra were recorded on a spectrophotometer (UV-2600, Shimadzu, Japan) using matched silica cuvettes with a path length of 10 mm. The temperature was maintained at 25 ± 0.1 °C in a water bath. In the experiments studying dye–dye interactions, the concentration of one dye was kept constant at 1.0×10^{-5} mol L^{-1}, while the concentration of the other dye varied from 0.0–1.0×10^{-5} mol L^{-1}.

2.3 The method of continuous variations

The method of continuous variations, also called Job's method, was used to determine the stoichiometric composition of the dye complexes in solution. This method is commonly used for dye–surfactant interaction studies.[11,12] A Job's plot was obtained by mixing different volume fractions of equimolar solutions of BB22 and RY86 with an initial concentration of 1.0×10^{-5} mol L^{-1}, then reading the absorbances of the mixtures at 600 nm, and plotting the corrected absorbances (ΔE) of these mixtures *versus* their volume fractions. ΔE represents the difference between the measured absorbance, E_{exp}, and the theoretical absorbance, E_{theo}.

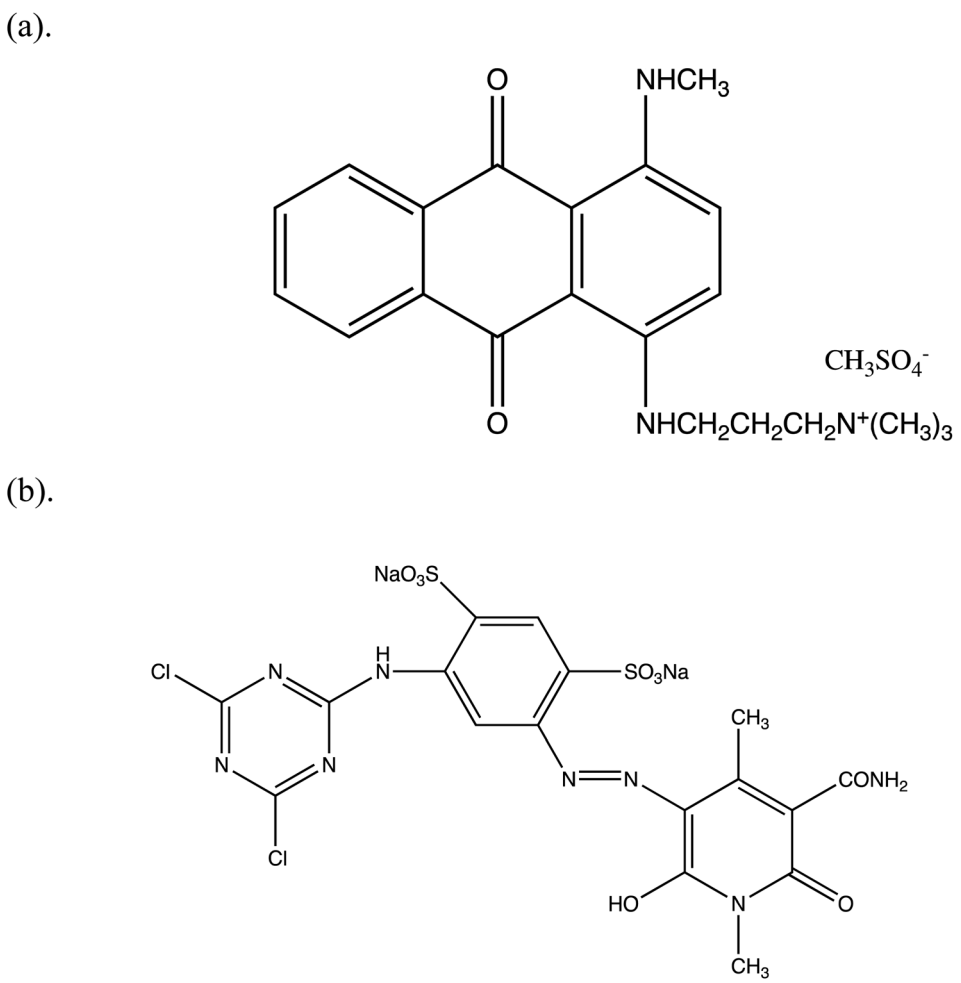

Fig. 1 Chemical structure of (a) basic blue 22 (BB22, M_{BB22} = 352.5 g mol^{-1}) and (b) reactive yellow 86 (RY86, M_{RY86} = 653.3 g mol^{-1}).

$$\Delta E = E_{exp} - E_{theo} \quad (1)$$

E_{theo} represents the absorbance of the mixture if no reaction occurs, and is equal to the sum of the absorbance of BB22 and RY86 individually. E_{exp} is the sum of absorbances of all compounds existing in solution, including BB22, RY86, and their complex, B_xR_y.

$$E_{theo} = \varepsilon_B C_B^0 X_B + \varepsilon_R C_R^0 (1 - X_B) \quad (2)$$

$$E_{exp} = \varepsilon_B C_B + \varepsilon_R C_R + \varepsilon_{B_xR_y} C_{B_xR_y} \quad (3)$$

where ε_B and ε_R are the molar extinction coefficients of BB22 and RY86, C_B^0 and C_R^0 are the concentrations of the BB22 and RY86 stock solutions, X_B is the volume ratio of the BB22 stock solution in the mixture, $\varepsilon_{B_xR_y}$ is the molar extinction coefficient of the complex, and C_B, C_R, and $C_{B_xR_y}$ are the concentrations of the species in the mixture, respectively.

The absorption of the mixtures was measured at the maximum absorption peak of BB22, at which RY86 showed nearly no absorption. Therefore, ΔE could be calculated by using the following equation:

$$\Delta E = E_{exp} - \varepsilon_B C_B^0 X_B \quad (4)$$

By plotting ΔE *vs.* X_B, the stoichiometric ratio of BB22 and RY86 in the complex were obtained as the minimum and maximum in the plot, respectively.

2.4 Chemical coagulation process

The optimal coagulation based on pH value and the optimal coagulant dose was determined by a jar test procedure. The pH of the solution was measured with a pH meter (PHS-3C, Leici, China). Then, 500 mL of dye solution was placed on a mechanical stirrer and the pH was adjusted. The coagulant and dye solution were mixed for 1 min at 300 rpm. This was followed by a 10 min period of slow stirring at 50 rpm and 30 min of sedimentation. After settling, the supernatant was centrifuged for 5 min to obtain a clear liquid. Because pH could affect the molecular structure of the dyes, which would change the absorbance of the solutions,[13] the pH of the supernatant was adjusted to 7.0 before sending it for UV analysis. The concentrations of BB22 and RY86 in both the single-dye solution and the mixed-dye solutions were 1.0×10^{-4} mol L^{-1}.

2.5 Ultrafiltration process

The ultrafiltration (UF) experiments were carried out in a dead-end cell filtration system fitted with a UF membrane, which had an effective membrane area of 12.6 cm^2. The UF membranes were made from PES and were conditioned in deionized water for 24 h before being used. In each experimental run, a fresh membrane was used. Dye solutions of BB22, RY86, and mixtures of both were prepared and incubated for 24 h before the filtration experiments. For each filtration experiment, the permeate samples were collected at specified volume intervals and the experiments were stopped when the total permeate volume reached 300 mL. The dye concentration in the permeate sample was analyzed by spectral measurements. Flux tests were performed at an operating pressure of 1.0 bar. The rejection rate (R) of the dye was calculated using eqn (5).

$$R = \frac{C_F - C_P}{C_F} \times 100\% \quad (5)$$

where C_F and C_P are the concentrations of dye in the feed and permeate solutions, respectively.

The permeate flux was calculated using eqn (6) as follows:

$$J = \frac{V}{S \times t} \quad (6)$$

where V is the volume of permeate, S is the effective area of the membrane, and t is the permeate collection time. All filtration experiments were conducted at room temperature.

3. Results and discussion

Both ionic surfactants and ionic dyes are amphiphiles, in which they have bulky, hydrophobic non-ionic moieties attached to hydrophilic ionic head groups. Thus, ionic dyes reveal some physicochemical properties similar to ionic surfactants. They can absorb at the air–water interface, leading to a reduction of the surface tension, and can self-aggregate to form dimers, trimers, or higher aggregates in water.[14] However, ionic dyes are unable to form complex micelle structures since they have no pendant alkyl groups.[15] Therefore, the interaction between different dyes may be studied in similar manners using the theories that describe dye–surfactant interactions; more specifically, when surfactants are at a premicellar concentration range.

To avoid interference problems due to the overlap of absorption peaks, BB22 and RY86 were chosen for the following experiments, since their characteristic absorption peaks are close to UV and IR regions, respectively. The dyes were used in a low concentration range to achieve a suitable absorbance range and avoid self-aggregation, which is well known to occur at high concentrations.[16]

3.1 UV-visible spectroscopic study on dye–dye interactions

To examine the interactions between ionic dyes with opposite charges, a series of solutions of RY86 and BB22 were prepared. The concentration of one dye fixed at 0.01 mM, while the concentration of the other dye gradually increased from 0.002 mM to 0.01 mM. The absorption spectrum was recorded in 0.5 nm intervals from 350 to 750 nm at 298 K. The wavelength of maximum absorption (λ_{max}) of RY86 and BB22 were 423 and 600 nm, respectively, and the Lambert–Beer law was valid for both dyes in the experimental concentration range. As shown in Fig. 2(a), when the RY86 concentration increased, a blue shift in the absorption peak (λ_{max} from 600 nm to 593 nm), accompanied by a pronounced reduction in the absorbance was observed for the spectrum of BB22. However, as the BB22 concentration increased, the spectral changes of RY86 were minimal, as shown in Fig. 2(b). To determine the stoichiometric composition of the dye complexes in solution, a Job's plot for the BB22/RY86 mixtures at different concentrations was drawn, as shown in Fig. 3. It can be seen that a minimum was obtained at approximately $X = 0.66$.

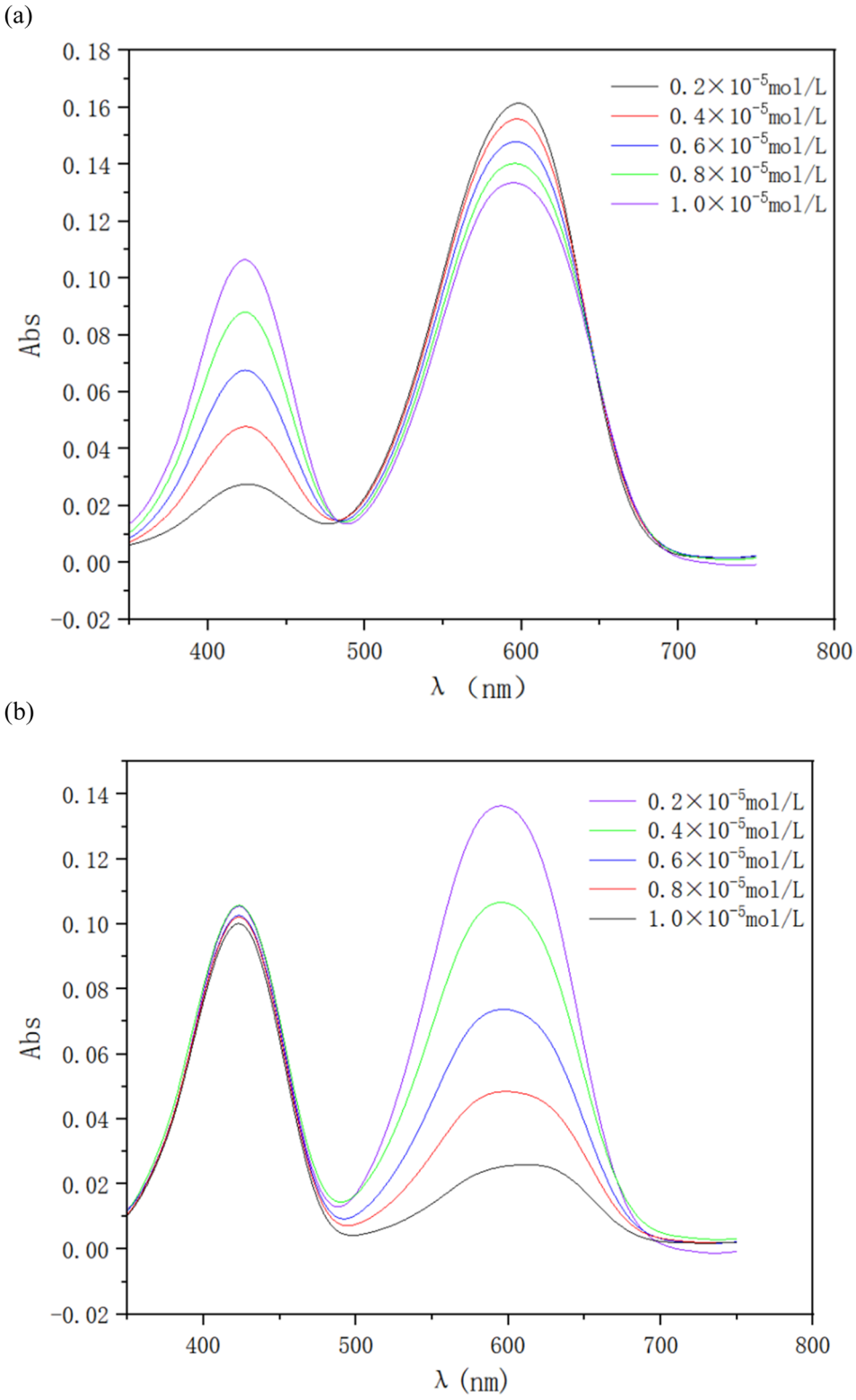

Fig. 2 (a) Absorption spectra of 1.0×10^{-5} mol L^{-1} aqueous BB22 in the presence of different concentrations of RY86 (0.2×10^{-5}, 0.4×10^{-5}, 0.6×10^{-5}, 0.8×10^{-5}, and 1.0×10^{-5} mol L^{-1}) at 25 °C. (b) Absorption spectra of 1.0×10^{-5} mol L^{-1} aqueous RY86 in the presence of different concentrations of BB22 (0.2×10^{-5}, 0.4×10^{-5}, 0.6×10^{-5}, 0.8×10^{-5}, and 1.0×10^{-5} mol L^{-1}) at 25 °C.

Similar to the interaction between oppositely charged ionic dyes and ionic surfactants in the premicellar concentration range, when the cationic BB22 was mixed with the anionic RY86, the molecules were attracted to each other and formed ion pairs under a combination of long-range electrostatic attractions and short-range hydrophobic forces.[14,17] Job's plot in

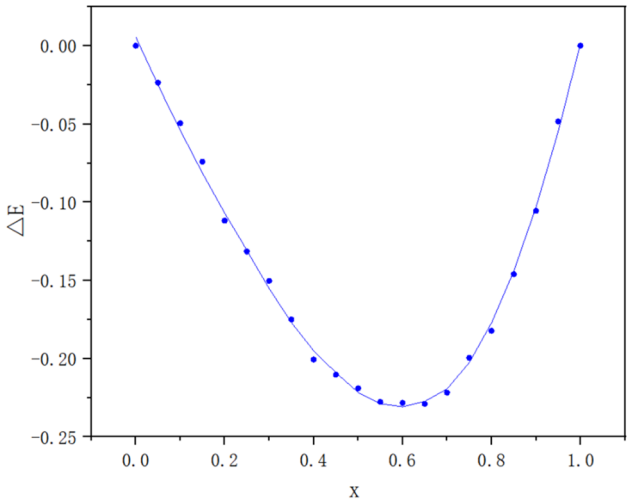

Fig. 3 Job's plot of BB22 and RY86 in aqueous solutions at 25 °C.

Fig. 3 indicates that a 2 : 1 complex, B_2R, was formed in the range of the concentrations studied. The coincident appearance of a decrease in absorbance and a shift in the absorption peak often indicates self-aggregation of the dye molecules.[14,18,19] Therefore, the spectra in Fig. 2(a) mostly likely indicated that the two BB22 ions in the ion pair were aggregated as a dimer. This is because the electrostatic repulsion between the two BB22 ions was suppressed in the ion pair; moreover, BB22 is highly hydrophobic and the main structure of the molecule is a large, planar, and rigid anthraquinone ring, which easily forms intermolecular π–π stacking. This induced self-aggregation of dyes was also found when ionic dyes were mixed with oppositely charged ionic surfactants at the pre-micellar concentration range.[19–21] In addition, when dyes are self-aggregated, they form H-aggregates if the chromophores are arranged in a parallel structure and J-aggregates if they are arranged in a head-to-tail structure. Compared to the monomer, the H- and J-aggregates are characterized by a blue and red shift in the absorption peak.[22] Thus, the blue shift of the BB22 absorption peak shown in Fig. 2(a) indicated the formation of H-aggregates. In contrast, as shown in Fig. 2(b), the addition of BB22 had no significant effect on the morphology of RY86 in solution. This is because RY86 has hydrophilic hydroxyl and amino groups on the molecule, resulting in a weak hydrophobic effect. Moreover, its three aromatic rings are poorly coplanar, making intermolecular π–π stacking difficult. In summary, when cationic BB22 and anionic RY86 were mixed in an aqueous solution, ion pairs were formed. The basic unit structure of the ion pair was two BB22 cations self-aggregated to form an H-aggregate, mainly through hydrophobic interactions and van der Waals forces, and one RY86 anion surrounded the aggregate mainly through electrostatic attractions.

To investigate the interactions between dyes with the same charge, BB22 was added to a cationic yellow X-8GL solution and RY86 to a reactive brilliant blue KN-R solution. As expected, no significant changes were detected in the intensity, shape, or location of the absorption peaks. This is because the electrostatic repulsion forces between the same-charged dyes were stronger than other interactions, such as hydrophobic interactions and van der Waals forces, which prevented the dye molecules from becoming close to each other.[18,19]

3.2 Effects of dye–dye interactions on ultrafiltration

Ultrafiltration is a membrane separation technology used mainly for the separation of macromolecules and colloids from a solution, in which the molecular weight of the solute to be separated generally needs to be in the thousands of daltons. Therefore, ultrafiltration technology is often unable to separate dye pollutants from textile industry wastewater effectively. The main reason is that molecular weights of dyes are much lower than MWCO of the ultrafiltration membranes.[23] Some studies have been carried out in which chemicals were added to a solution to interact with dye molecules and eventually form macromolecular complexes larger than the ultrafiltration membrane pores, thus trapping the complexes. These studies include polymer-enhanced ultrafiltration, which is based on complexing dye molecules with water-soluble high molecular weight polymers[24] and micellar-enhanced ultrafiltration, in which dye molecules dissolve in large-size micelles formed when surfactant concentrations exceed their critical micelle concentration.[25] In this study, it is found that the interaction between dyes with opposite charges had a large influence on ultrafiltration treatment.

PES is one of the most widely used membrane materials in the wastewater treatment industry since it has a wide temperature range, wide pH tolerance, and mechanical strength.[26,27] An PES UF membrane with an MWCO of 10 kDa was used to filter the single-dye solutions of BB22 and RY86 at a concentration of 1.0×10^{-5} mol L^{-1}, and the rejection of dye was recorded *versus* permeate volume, as shown in Fig. 4. At the beginning of the filtration the rejection of BB22 reached 86.5% and then dropped rapidly to 12.4% at the end of filtration. The rejection of RY86 was much lower at about 10% at the beginning of filtration, and then almost zero during the rest of the filtration. Since the BB22 and BY86 molecules are much smaller than the membrane pores, and their self-aggregation does not occur at these low concentrations, the rejection at the beginning of filtration could be attributed to the adsorption of dye molecules at the surface and pore walls of the membrane.[28,29] The difference in adsorption between BB22 and RY86 on the UF membrane was mainly due to their opposite charges. Although PES is a non-charged material, many studies have demonstrated that PES membranes have a negative charge over a certain pH range.[26,30,31] The origin of the negative charge was caused by the preferential adsorption of electrolyte ions in aqueous environments, particularly the preferential adsorption of hydroxide ions. Therefore, the membrane relatively effectively adsorbed cationic BB22 through electrostatic attraction.

However, when BB22 and RY86 were mixed and then filtered under the same experimental conditions, the dye rejection changed greatly, as shown in Fig. 4. Compared to the single-dye solution, the rejection of BB22 in the mixed solution increased to 96.2% and remained stable for the first 200 mL of filtration, and then dropped slowly to 74.8% by the end of the experiment.

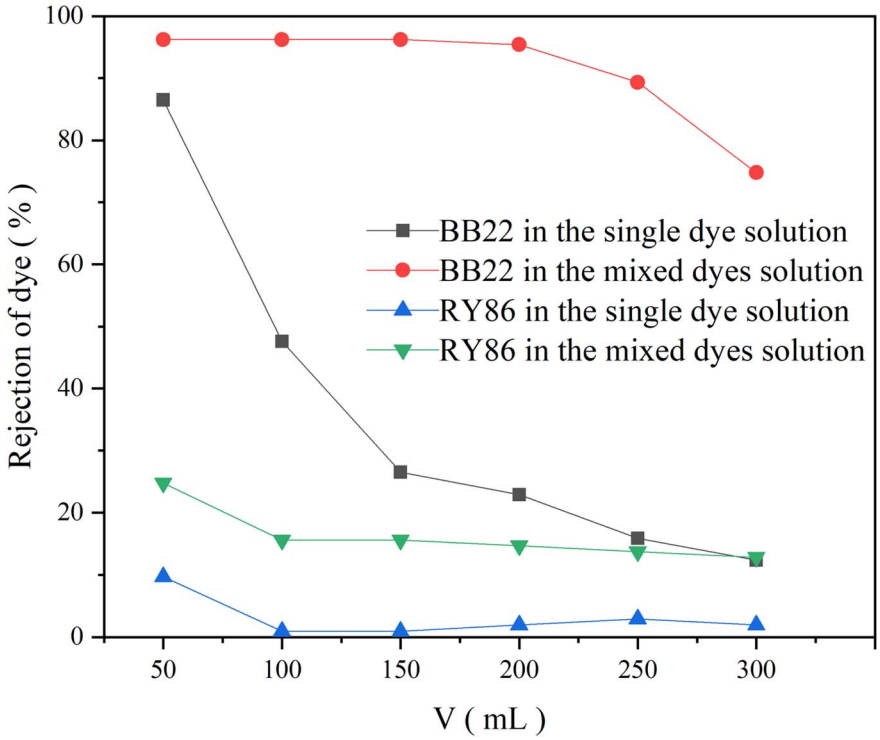

Fig. 4 The rejection of BB22 and RY86 in the single-dye solutions and the mixed-dye solution by UF membranes with an MWCO of 10 kDa.

The rejection rate of RY86 also increased to a certain extent, and the overall increase was about 15.0%. This increase in dye rejection during ultrafiltration also occurred after mixing the dye in the pre-micelle concentration range with a surfactant that had an opposite charge.[4,32,33]

This phenomenon might be caused by a combination of the following: (i) as previously mentioned, when BB22 and RY86 are mixed, they are attracted to each other due to electrostatic attraction and induce self-aggregation of BB22. The BB22 aggregates have more positive charges, so they are more easily adsorbed on the negatively charged PES membrane during the ultrafiltration process. The adsorbed BB22 aggregates then bind the anionic RY86 in the aqueous solution, which increases the rejection rate of RY86. (ii) This polarization effect increases the concentration of dyes on the membrane surface, which further promotes dye aggregation.[34] Aggregates may increase in size and become similar to or larger than the membrane pore size, thereby blocking the membrane pores or depositing on the membrane surface.[29] Fig. 5 shows the results of the use of UF membranes with an MWCO of 5 kDa, 10 kDa, and 30 kDa to filter the mixed-dye solution, which showed that, with a smaller membrane pore size, the rejection of BB22 increased, which also supports this speculation.

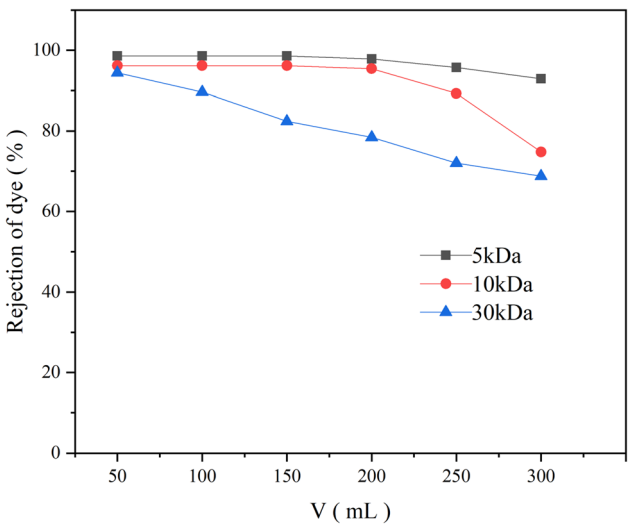

Fig. 5 The rejection of BB22 in the mixed-dye solution by UF membranes with different MWCOs.

While mixing the dyes increased the rejection during ultrafiltration, it decreased the permeate flux of the dye solution, as shown in Fig. 6. This is because the more dyes adsorbed or deposited in the membrane pores or on its external surface, the more serious the membrane fouling. In addition, during the progression of ultrafiltration, the membrane flux was gradually reduced, indicating that fouling was aggravated during the UF process.

3.3 Effect of dye–dye interactions on chemical coagulation

Chemical coagulation is one of the most commonly used technologies for the treatment of dye wastewater.[35,36] It is accomplished by adding chemicals to wastewater to alter the physical state of dissolved and suspended dye contaminants, which are ultimately removed by sedimentation.[5] It produces good decolorization for most dye wastewater but is ineffective for

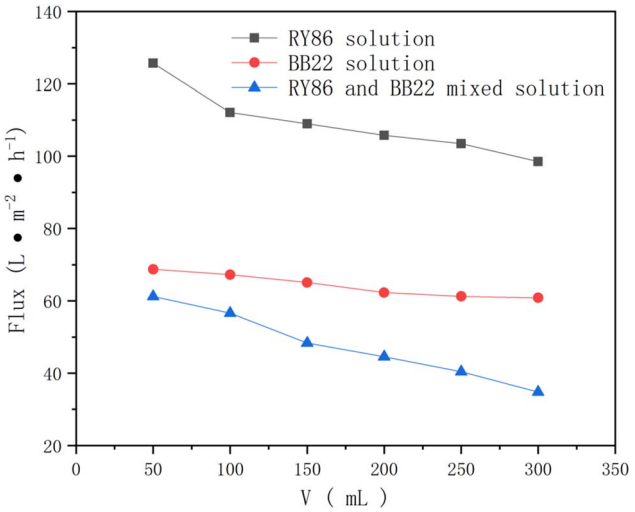

Fig. 6 The permeate flux of the single-dye solution and the mixed-dye solution by UF membranes with an MWCO of 10 kDa.

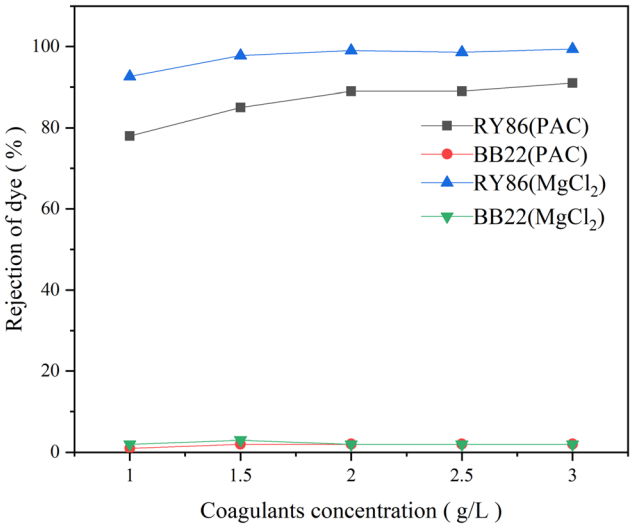

Fig. 8 The rejection rate of BB22 and RY86 in the single-dye solutions with $MgCl_2$ and PAC coagulation at different coagulant doses.

some soluble dyes.[37] Many studies have been conducted on various factors affecting chemical coagulation, including dye types, coagulant types, coagulant doses, and pH values.[6] However, very limited work has been carried out on the effect of intermolecular interactions of multiple dyes of different classes.[5] In this study, it is found that the intermolecular interaction between dyes with opposite charges had a large influence on chemical coagulation.

First, two commonly used metal coagulants, $MgCl_2$ and PAC, were tested for the coagulation of the single-dye solutions of both BB22 and RY86, and optimization experiments on the coagulation pH and coagulant doses were carried out. The results are as shown in Fig. 7 and 8. Under certain experimental conditions, both $MgCl_2$ and PAC exhibited excellent removal effects for RY86 with a removal rate over 98%. However, neither $MgCl_2$ nor PAC effectively removed BB22, and the removal rate was below 20% throughout the experiment. It is known that charge neutralization plays an important role when coagulating dyes with metal coagulants.[38] When the metal coagulant was added to the solution, it hydrolyzed and provided a large absorptive surface area with a positive electrostatic charge, which then attracted the anionic RY86 and repelled the cationic BB22. It can also be seen from Fig. 8 that pH had a great influence on the coagulation process. The removal rate of RY86 first increased and then decreased as the pH increased, while the removal rate of BB22 increased slowly as the pH increased. This is because when the solution pH was too low, the metal coagulant could not be fully hydrolyzed, while as the pH increased, the hydrolysate surface became less positively charged and possibly negatively charged when the pH was above the isoelectric point.[5,13] Coagulant doses had a certain influence on the removal of dyes, as shown in Fig. 8. With increasing doses, removal of RY86 increased at first and then remained largely unchanged. However, the removal rate of BB22 was consistently very low, which further confirmed the importance of the charge neutralization mechanism. In addition, it was reported that the –OH functional group in the dye molecules can react with magnesium ions and lead to the formation of magnesium hydroxide precipitates,[13,38] which may be the reason $MgCl_2$ exhibited a better removal effect on RY86.

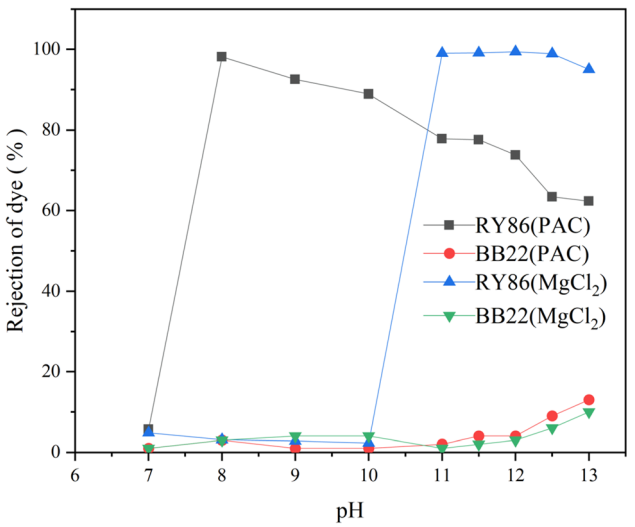

Fig. 7 The rejection rate of BB22 and RY86 in the single-dye solutions with $MgCl_2$ and PAC coagulation at different pH values.

Then, BB22 and RY86 were mixed in equimolar ratios, and coagulation experiments were performed under the optimized pH and doses obtained above, with the results shown in Fig. 9. Mixing the dyes had a substantial impact on the removal effect. The removal of BB22 increased dramatically—from 2.8% to 28.0% with PAC, and from 3.3% to 67.5% with $MgCl_2$. This enhancement might be due to RY86 binding to BB22 on the coagulant surface. Since RY86 has two negatively charged sulfonate groups, it might be that one is attracted to the surface of the metal coagulant, while the other binds cationic BB22 aggregates at the same time. In addition, the –OH functional

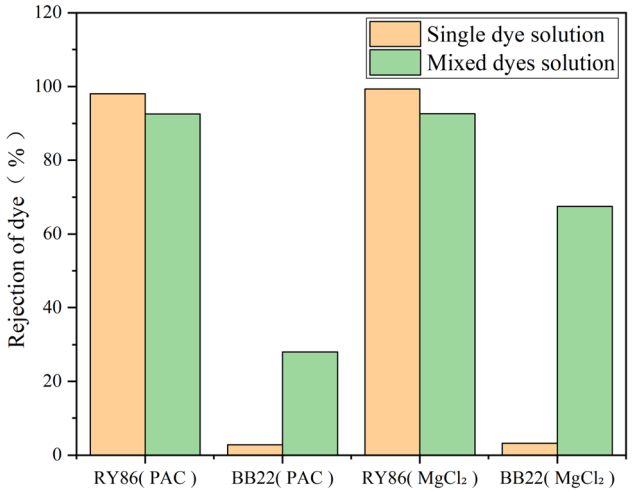

Fig. 9 The removal rate of BB22 and RY86 in the single-dye solutions and the mixed-dye solution with $MgCl_2$ and PAC coagulation.

group in RY86 may react with the magnesium ions and be fixed on the surface of the $MgCl_2$ hydrolysate, so that there are two sulfonate groups for binding BB22, which also explains why $MgCl_2$ exhibited better removal of BB22 in the mixed solution. However, it should be noted that the removal of RY86 in the mixed solution decreased slightly—from 98.1% to 92.6% with PAC, and from 99.4% to 92.3% with $MgCl_2$. This is because part of RY86 bound to BB22 and remained in the bulk solution.

It can be seen from the above results that mixing dyes with opposite charges had a great impact on chemical coagulation and membrane separation. With these treatment techniques, electrostatic attraction played an important role. For example, positively charged coagulant hydrolysates adsorbed dyes with a negative charge, while negatively charged membrane surfaces adsorbed dyes with a positive charge. When the dyes with opposite charges were mixed, they approached each other due to electrostatic attraction, so that the dyes that could be adsorbed by the removal reagents bound the oppositely charged dyes at the same time. The result was the removal of the oppositely charged dye, which could not originally be effectively removed, now showed increased removal. Similar results were found by Li *et al.* when they developed a zirconium-metalloporphyrin mesoMOF absorbent for the removal of cationic methyl orange and anionic methylene blue, in which they proposed the same mechanism to explain the mutual enhancement of adsorption in a mixture dye solution.[39] Thus, it is possible to remove dyes that are difficult to remove by conventional methods, such as basic dyes,[40] by mixing with oppositely charged dyes and even to achieve simultaneous removal of anionic and cationic dyes, which was considered a challenge in previous studies.[41]

4. Conclusions

In conclusion, this study provides insights into the realm of dye–dye interactions and their implications for wastewater treatment strategies. The key findings of this study are two-fold. First, the study demonstrates that when cationic and anionic dyes are mixed, they form ion pairs and aggregates due to the interplay of electrostatic attractions and hydrophobic forces. Second, these interactions between dyes carrying opposite charges significantly enhance the efficiency of treatment methods. By exploiting these interactions, both chemical coagulation and ultrafiltration processes achieve heightened removal efficiencies. For example, anionic dyes increase adsorption on the surface of anionic UF membranes by forming ion pairs and aggregates with cationic dyes. These findings have significant implications for wastewater treatment practices. By capitalizing on the principles of opposite-charged dye interactions, industries can design more efficient and sustainable methods for tackling dye contamination.

Conflicts of interest

There are no conflicts to declare.

Acknowledgements

This study was supported by the Natural Science Foundation of Fujian Province of China (No. 2022J011098), Major Program of Qingyuan Innovation Laboratory (No. 00122003), Quanzhou Science and Technology Program (No. 2019C107) and Young and Middle-aged Teacher Education Research Project of the Department of Education of Fujian Province (No. JT180369).

References

1 H. Zollinger, Syntheses, properties and applications of organic dyes and pigments, *Colour Chemistry*, VCH Publishers, Weinheim, 2nd edn, 1991, p. 496.
2 J. Dasgupta, *et al.*, Remediation of textile effluents by membrane based treatment techniques: a state of the art review, *J. Environ. Manage.*, 2015, **147**, 55–72.
3 M. Bilal, *et al.*, Mutagenicity and cytotoxicity assessment of biodegraded textile effluent by Ca-alginate encapsulated manganese peroxidase, *Biochem. Eng. J.*, 2016, **109**, 153–161.
4 J.-H. Huang, *et al.*, Micellar-enhanced ultrafiltration of methylene blue from dye wastewater via a polysulfone hollow fiber membrane, *J. Membr. Sci.*, 2010, **365**(1–2), 138–144.
5 A. K. Verma, R. R. Dash and P. Bhunia, A review on chemical coagulation/flocculation technologies for removal of colour from textile wastewaters, *J. Environ. Manage.*, 2012, **93**(1), 154–168.
6 A. Y. Zahrim, C. Tizaoui and N. Hilal, Coagulation with polymers for nanofiltration pre-treatment of highly concentrated dyes: a review, *Desalination*, 2011, **266**(1–3), 1–16.
7 T. Shindhal, *et al.*, A critical review on advances in the practices and perspectives for the treatment of dye industry wastewater, *Bioengineered*, 2021, **12**(1), 70–87.
8 W. Xiao, *et al.*, Adsorption of organic dyes from wastewater by metal-doped porous carbon materials, *J. Cleaner Prod.*, 2021, **284**, 124773.

9 B. Parmar, *et al.*, Recent advances in metal-organic frameworks as adsorbent materials for hazardous dye molecules, *Dalton Trans.*, 2021, **50**(9), 3083–3108.
10 T. U. Rashid, *et al.*, Sustainable wastewater treatment via dye–surfactant interaction: a critical review, *Ind. Eng. Chem. Res.*, 2020, **59**(21), 9719–9745.
11 S. Gokturk and M. Tuncay, Dye-surfactant interaction in the premicellar region, *J. Surfactants Deterg.*, 2003, **6**(4), 325–330.
12 P. Forte-Tavčer, Interactions between some anionic dyes and cationic surfactants with different alkyl chain length studied by the method of continuous variations, *Dyes Pigm.*, 2004, **63**(2), 181–189.
13 B. Y. Gao, *et al.*, Color removal from dye-containing wastewater by magnesium chloride, *J. Environ. Manage.*, 2007, **82**(2), 167–172.
14 M. Rashidi-Alavijeh, *et al.*, Intermolecular interactions between a dye and cationic surfactants: effects of alkyl chain, head group, and counterion, *Colloids Surf., A*, 2011, **380**(1), 119–127.
15 J. Oakes and S. Dixon, Physical interactions of dyes in solution – influence of dye structure on aggregation and binding to surfactants/polymers, *Rev. Prog. Color. Relat. Top.*, 2004, **34**(1), 110–128.
16 M. G. Neumann and M. H. Gehlen, The interaction of cationic dyes with anionic surfactants in the premicellar region, *J. Colloid Interface Sci.*, 1990, **135**(1), 209–217.
17 B. Gohain and R. K. Dutta, Premicellar and micelle formation behavior of dye surfactant ion pairs in aqueous solutions: deprotonation of dye in ion pair micelles, *J. Colloid Interface Sci.*, 2008, **323**(2), 395–402.
18 M. Bielska, A. Sobczyńska and K. Prochaska, Dye–surfactant interaction in aqueous solutions, *Dyes Pigm.*, 2009, **80**(2), 201–205.
19 S. Ghosh, *et al.*, Spectroscopic investigation of interaction between crystal violet and various surfactants (cationic, anionic, nonionic and gemini) in aqueous solution, *Fluid Phase Equilib.*, 2012, **332**, 1–6.
20 M. Sarkar and S. Poddar, Studies on the Interaction of Surfactants with Cationic Dye by Absorption Spectroscopy, *J. Colloid Interface Sci.*, 2000, **221**(2), 181–185.
21 M. Ekaterina, *et al.*, Photoacoustic lifetime contrast between methylene blue monomers and self-quenched dimers as a model for dual-labeled activatable probes, *J. Biomed. Opt.*, 2013, **18**(5), 1–9.
22 B. Heyne, Self-assembly of organic dyes in supramolecular aggregates, *Photochem. Photobiol. Sci.*, 2016, **15**(9), 1103–1114.
23 H. Ouni and M. Dhahbi, Spectrometric study of crystal violet in presence of polyacrylic acid and polyethylenimine and its removal by polyelectrolyte enhanced ultrafiltration, *Sep. Purif. Technol.*, 2010, **72**(3), 340–346.
24 Y. Huang and X. Feng, Polymer-enhanced ultrafiltration: fundamentals, applications and recent developments, *J. Membr. Sci.*, 2019, **586**, 53–83.
25 M. Schwarze, Micellar-enhanced ultrafiltration (MEUF) – state of the art, *Environ. Sci.: Water Res. Technol.*, 2017, **3**(4), 598–624.
26 L. Zheng, *et al.*, Adsorption and recovery of methylene blue from aqueous solution through ultrafiltration technique, *Sep. Purif. Technol.*, 2009, **68**(2), 244–249.
27 A. Aouni, *et al.*, Reactive dyes rejection and textile effluent treatment study using ultrafiltration and nanofiltration processes, *Desalination*, 2012, **297**, 87–96.
28 X. Tan, *et al.*, Decolorization of dye-containing aqueous solutions by the polyelectrolyte-enhanced ultrafiltration (PEUF) process using a hollow fiber membrane module, *Sep. Purif. Technol.*, 2006, **52**(1), 110–116.
29 E. Oyarce, *et al.*, Polyelectrolytes applied to remove methylene blue and methyl orange dyes from water via polymer-enhanced ultrafiltration, *J. Environ. Chem. Eng.*, 2021, **9**(6), 106297.
30 Y. He, *et al.*, Effect of operating conditions on separation performance of reactive dye solution with membrane process, *J. Membr. Sci.*, 2008, **321**(2), 183–189.
31 W. R. Bowen, T. A. Doneva and H.-B. Yin, Separation of humic acid from a model surface water with PSU/SPEEK blend UF/NF membranes, *J. Membr. Sci.*, 2002, **206**(1–2), 417–429.
32 H. Ngang, *et al.*, Preparation of PVDF–TiO_2 mixed-matrix membrane and its evaluation on dye adsorption and UV-cleaning properties, *Chem. Eng. J.*, 2012, **197**, 359–367.
33 N. Zaghbani, A. Hafiane and M. Dhahbi, Separation of methylene blue from aqueous solution by micellar enhanced ultrafiltration, *Sep. Purif. Technol.*, 2007, **55**(1), 117–124.
34 N. Florence and H. Naorem, Dimerization of methylene blue in aqueous and mixed aqueous organic solvent: a spectroscopic study, *J. Mol. Liq.*, 2014, **198**, 255–258.
35 Y. Anjaneyulu, N. Sreedhara Chary and D. Samuel Suman Raj, Decolourization of industrial effluents – available methods and emerging technologies – a review, *Rev. Environ. Sci. Bio/Technol.*, 2005, **4**(4), 245–273.
36 M. C. Collivignarelli, *et al.*, Treatments for color removal from wastewater: state of the art, *J. Environ. Manage.*, 2019, **236**, 727–745.
37 F. I. Hai, K. Yamamoto and K. Fukushi, Hybrid treatment systems for dye wastewater, *Crit. Rev. Environ. Sci. Technol.*, 2007, **37**(4), 315–377.
38 F. McYotto, *et al.*, Effect of dye structure on color removal efficiency by coagulation, *Chem. Eng. J.*, 2021, **405**, 126674.
39 H. Li, *et al.*, Enhanced adsorptive removal of anionic and cationic dyes from single or mixed dye solutions using MOF PCN-222, *RSC Adv.*, 2017, **7**(27), 16273–16281.
40 M. Joshi, R. Bansal and R. Purwar, Colour removal from textile effluents, *Indian J. Fibre Text. Res.*, 2004, **29**, 239–259.
41 A. Ayati, *et al.*, Emerging adsorptive removal of azo dye by metal–organic frameworks, *Chemosphere*, 2016, **160**, 30–44.